Composites: Part B 42 (2011) 809–818

Contents lists available at ScienceDirect

Composites: Part B

journal homepage: www.elsevier.com/locate/compositesb

Synthesis, swelling and responsive properties of a new composite hydrogel based on hydroxyethyl cellulose and medicinal stone

Wenbo Wang, Jiang Wang, Yuru Kang, Aiqin Wang *

Center for Eco-Material and Green Chemistry, Lanzhou Institute of Chemical Physics, Chinese Academy of Sciences, Lanzhou 730000, PR China

ARTICLE INFO

Article history:
Received 29 September 2010
Received in revised form 15 December 2010
Accepted 21 January 2011
Available online 27 January 2011

Keywords:
A. Polymer-matrix composites (PMCs)
D. Thermal analysis

ABSTRACT

In this study, a series of pH- and saline-responsive composite hydrogels were prepared by a facile free-radical graft copolymerization amongst hydroxyethyl cellulose (HEC), sodium acrylate (NaA) and medicinal stone (MS). Fourier transform infrared spectroscopy (FTIR) and Thermogravimetric/Differential thermal analysis (TG/DTA) confirmed NaA was grafted onto HEC and MS participate in polymerization, and presented the improved thermal stability. Field emission scanning electron micro-scope (FESEM), Energy dispersive spectroscopy (EDS), Elemental map (EM) and Transmission electron microscopy (TEM) analyses revealed a better distribution of MS in the HEC-*g*-PNaA matrix. Introducing 10 wt% MS greatly enhanced the swelling capacity by 400% (from 162 to 810 g/g), and also enhanced by 117% (from 162 to 352 g/g) even MS content reached 50 wt%. Also, the initial swelling rate was improved by incorporating MS, but decreased with enhancing the ion strength. The highly reversible On–Off switching pH- and saline-responsive region of the hydrogel was clearly extended after forming composite. In addition, the intriguing "overflowing" swelling behaviour was observed in aqueous solution of dimethyl sulfoxide (DMSO).

1. Introduction

Organic–inorganic composite materials based on natural polymers and inorganic clay minerals have recently received considerable attentions in both academic research and industrial application due to their excellent hybrid properties superior to each individual component as well as environmentally friendly characteristics [1–3]. Hydrogels are slightly crosslinked hydrophilic functional polymer materials with unique 3D network structure and water-swellable properties. Owing to the advantages of hydrogel as a soft material over other materials, it has been extensively applied in many fields such as hygienic products [4], agriculture [5,6], wastewater treatment [7–10], carrier of catalyst [11,12], drug-delivery systems [13,14] and bioengineering material [15].

With the increasing environmental topics and the expanding application of hydrogels, the responsive properties of such materials are attractive and desirable apart from their swelling characteristics [16]. Many kinds of raw materials were taken as the matrix for the fabrication of functional hydrogels [17–20], and the renewable, biodegradable, non-toxic and biocompatible natural polysaccharides are preferred, effective and potential due to their excellent performance and environmentally friendly characteristics [21]. Thus far, various polysaccharides including starch [19,22], cellulose [20,23], sodium alginate [24,25], chitosan [26], guar gum [27,28], carrageenan [29] and gelatin [30], etc. have been focused and used for the preparation of environmentally friendly responsive hydrogels. Amongst them, cellulose and its derivatives showed unique advantages because they are the most abundant natural polysaccharide with low cost, better biodegradability and biocompatibility. Hydroxyethyl cellulose (HEC) is a representative derivative of cellulose with excellent water solubility and biocompatibility. The excellent properties of HEC allow it to be used in many biotechnological, biophysical and industrial fields. Because of the existence of abundant reactive –OH groups on the HEC chains, HEC is liable to be modified by grafting polymerization with hydrophilic vinyl monomers to derive new materials with improved properties [31]. Medicinal Stone (MS) is a special igneous rock composed of silicic acid, alumina oxide and more than 50 kinds of constant and trace elements. The main chemical composition of MS is aluminum metasilicate including $KAlSi_3O_8$, $NaAlSi_3O_8$, $CaAl_2Si_2O_8$, $MgAl_2Si_2O_8$ and $FeAl_2Si_2O_8$, etc. In such a structure, silica (SiO_2) presents regular tetrahedron with a [SiO_4] configuration, and shows a three-dimensional stereo-structure in which aluminum coordinates through oxo-bridging in a moiety of its structures. By virtue of the better porousness, multicomponent characteristic, biological activity and safety, MS has been extensively applied in food science, medicine, daily chemical industry, environmental sanitation and wastewater treatment, etc. [32]. However, little attention focuses on the application of MS as an inorganic additive of a composite hydrogel. So, the chemical composite of HEC and MS was expected to derive new kind of hydrogel

* Corresponding author. Tel.: +86 931 4968118; fax: +86 931 8277088.
E-mail address: aqwang@licp.cas.cn (A. Wang).

1359-8368/$ - see front matter © 2011 Elsevier Ltd. All rights reserved.
doi:10.1016/j.compositesb.2011.01.018

materials with improved network structure and comprehensive performance.

On the basis of the above background, in current work, the free-radical solution polymerization amongst HEC, NaA and MS was performed to fabricate a series of novel hydroxyethyl cellulose-*g*-poly(sodium acrylate)/medicinal stone (HEC-*g*-PNaA/MS) composite hydrogels. The structure, morphologies and thermal stability of the composite hydrogels were characterized by Fourier transform infrared spectroscopy (FTIR), Field emission scanning electron micro-scope (FESEM), Energy dispersive spectroscopy (EDS), Elemental map (EM), Transmission electron microscopy (TEM), Thermogravimetric/Differential thermal analysis (TG/DTA) techniques. The capacity and rate of swelling for the hydrogels were studied, and the enhanced pH- and saline-sensitive properties as well as the swelling behaviours of the hydrogels in the aqueous solutions of various salts, surfactants and hydrophilic organic solvents were also systematically evaluated.

2. Experimental

2.1. Materials

HEC (practical grade, viscosity 4000 cP) was purchased from Serva Feinbiochemica (Heidelberg, Germany). Acrylic acid (AA, chemically pure, Shanghai Shanpu Chemical Factory, Shanghai, China) was distilled under reduced pressure, and partially neutralized using NaOH solution before use. MS micro-powder (Chinese M-Stone Development Co., Ltd, NaiMan, Inner Mongolia, China) was milled and passed through a 320-mesh screen (<46 μm) prior to use, and the main chemical composition is SiO_2, 68.89%; Al_2O_3, 14.06%; Fe_2O_3, 3.61%; K_2O, 3.18%; Na_2O, 4.86%; CaO, 1.33%; MgO, 2.59%. Ammonium persulfate (APS, analytical grade) was purchased from Xi'an Chemical Reagent Factory (Xi'an, China) and was recrystallized from water before use. *N,N′*-methylene-*bis*-acrylamide (MBA, chemically pure) was purchased from Shanghai Chemical Reagent Corp. (Shanghai, China). Sodium oleate (NaOL, chemically pure) was from Sinopharm Chemical Reagent Co.Ltd (Shanghai, China). Dodecyltrimethylammonium (DTAB, chemically pure) was from Xiamen XM-Innovation Chemical Co., Ltd. (Xiamen, China). Other reagents used were of analytical grade and all solutions were prepared with distilled water.

2.2. Synthesis of HEC-g-PNaA/MS composite hydrogels

HEC (1.2 g) was dissolved in 33 mL distilled water in a 250-mL four-necked flask equipped with a reflux condenser, a mechanical stirrer, a nitrogen line and a thermometer. The solution was heated to 60 °C and purged with N_2 for 30 min to remove the dissolved oxygen. Afterward, 5 mL of aqueous solution of initiator APS (72.0 mg) was added and stirred for 10 min to generate free-radicals. After the reactants was cooled to 50 °C, the mixed solution containing AA (7.2 g, neutralized with 8.2 mL 8.0 mol/L NaOH solution), crosslinker MBA (14.4 mg) and MS powders (0, 0.45, 0.95, 2.05, 3.54 g, 5.60 g and 8.40 g) was added, and the temperature was slowly risen to 70 °C and maintained for 3 h to complete polymerization. The obtained gels were dried to constant weight at 70 °C, and the dried gels were ground and passed through 40 to 80 mesh sieve (180–380 μm).

2.3. Measurements of equilibrium swelling capacity and swelling kinetics

0.05 g of sample was immersed in excess of aqueous fluids (including distilled water, 0.9 wt% NaCl solution, organic solvents/water mixture solutions and the aqueous solutions of surfactants in this work) at room temperature for 4 h to achieve swelling equilibrium. The swollen gels were then separated from the solutions using a 100-mesh screen. After weighing the swollen gels, the equilibrium swelling capacities (Q_{eq}, g/g) of the hydrogels were derived from the mass change before and after swelling, and calculated using the following equation (Eq. (1)):

$$Q_{eq} = (w_s - w_d)/w_d \quad (1)$$

where w_d and w_s are the weights of the dry sample and the swollen sample, respectively. Q_{eq} was calculated as grams of water per gram of sample.

Swelling kinetics of the hydrogel in each media was measured as follows: an accurately weighed sample (about 0.05 g) was fully contacted with 300 mL aqueous solution. At certain time intervals, the swelling capacity of the sample at a given time (Q_t, g/g) was measured by weighing the swollen gel and calculated according to Eq. (1). In all cases three parallel samples were used and the averages were reported in this paper.

2.4. Evaluation of pH- and saline-responsive properties

The solutions with pHs 2.0 and 7.4 were adjusted by 0.1 M HCl and NaOH solutions. The pH values of solutions were determined by a pH meter (DELTA-320). The pH- and saline-responsive properties of the composite hydrogel was investigated in terms of its swelling and deswelling between pHs 7.4 and 2.0, between distilled water and 0.9 wt% NaCl solution, respectively. Typically, 0.05 g sample was placed in a 100-mesh sieve and fully contacted with pH 2.0 solution or 0.9 wt% NaCl solution until the equilibrium was reached. The wetted sample was then immersed in pH 7.4 solution or distilled water for a set period of time. Finally, the swollen composite hydrogel was filtered, weighed and its swelling capacity at a given moment can be calculated according to Eq. (1). The consecutive time interval is 15 min for each cycle, and the same procedure was repeated for five cycles. After each measurement, the used solution was renewed.

2.5. Measurements of the swelling capacity in organic solvents/water mixture solutions and the concentration difference of DMSO between gel network and external solution

The organic solvents/water mixture solutions (10, 20, 30, 40, 50, 60, 70 and 80 vol%) were prepared by dissolving calculated volumes of organic solvents (methanol, acetone or DMSO). A 0.05 g of sample was immersed in 200 mL of each mixture solution at room temperature for 4 h to achieve swelling equilibrium. The swollen gels were then separated from the solutions using a 100-mesh screen. After weighing the swollen gels, the equilibrium swelling capacities (Q_{eq}, g/g) of the hydrogels in organic solvents/water solutions were derived from the mass change before and after swelling and calculated using the equation (Eq. (1)).

The concentration difference of DMSO between swollen gel network and external solution was determined according to the following procedure. A set of standard solutions with the concentration of 10, 20, 30, 40, 50, 60 and 70 vol% were prepared, and the fluorescence intensity of *S* elements for each standard solution was determined and the standard curve (the fluorescence intensity (y) versus the concentration of *S* element (x)) was established ($y = 4088.33 + 0.1208x$, $R = 0.999$). By determining the fluorescence intensity of *S* elements for the swollen hydrogels and the filtrate, the corresponding concentration of *S* elements can be obtained. The concentration of DMSO for each sample can be calculated by converting the concentration of S elements.

2.6. Characterizations

FTIR spectra were recorded on a Nicolet NEXUS FTIR spectrometer in 4000–400 cm^{-1} region using KBr pellets. The samples were extracted with ethanol for 24 h before determination. The surface morphologies, Energy dispersive spectroscopy (EDS) and Elemental map (EM) of each sample was examined using a JSM-6701F field emission scanning electron micro-scope (JEOL) after coating the sample with gold film. The Transmission electron micrographs (TEM) were obtained using a JEM-2010 high-resolution transmission electron micro-scope (JEOL, Tokyo, Japan) at an acceleration voltage of 200 kV, the sample was ultrasonically dispersed in ethanol before observation. Thermogravimetric/Differential thermal analysis (TG/DTA) were performed using a Perkin-Elmer TGA-7 thermogravimetric analyzer (Perkin–Elmer Cetus Instruments, Norwalk, CT), with a temperature range of 30–750 °C at a heating rate of 10 °C/min using dry nitrogen purge at a flow rate of 50 mL/min.

3. Results and discussion

3.1. FTIR spectra

The FTIR spectra of HEC, HEC-*g*-PNaA, HEC-*g*-PNaA/MS and MS were shown in Fig. 1. It can be seen from Fig. 1a that the absorption band of HEC at 1015 cm^{-1} (stretching vibration of C–OH groups) disappeared after reaction, and the bands at 1119 and 1061 cm^{-1} and (asymmetrical stretching vibration of C–O–C) appeared in the spectra of HEC-*g*-PNaA and HEC-*g*-PNaA/MS. The new bands at 1708 cm^{-1} for HEC-*g*-PNaA and 1702 cm^{-1} for HEC-*g*-PNaA/MS (asymmetrical stretching vibration of –COOH), at 1568 cm^{-1} for HEC-*g*-PNaA and 1563 cm^{-1} for HEC-*g*-PNaA/MS (asymmetrical stretching vibration of $–COO^-$ groups), at 1455 and 1410 cm^{-1} (symmetrical stretching vibration of $–COO^-$ groups) appeared in the spectra of HEC-*g*-PNaA and HEC-*g*-PNaA/MS (Fig. 1b and c). This observation reveals that PNaA and HEC chains existed in the composite hydrogel. For proving the graft of NaA onto HEC, the TG-DTA curves of HEC, HEC-*g*-PNaA and HEC-*g*-PNaA/MS were presented (Fig. 2). It can be noticed that the positions of endothermic peaks and weight-loss rate have clearly changed after graft reaction, indicating that NaA has been grafted onto HEC backbone. The characteristic absorption bands of MS at 3619 cm^{-1} and 1633 cm^{-1} (stretching and bending vibration of (Si)O–H, respectively) can almost not be observed after reaction (Fig. 1b–d), and the absorption band of MS at 1034 cm^{-1} (stretching vibration of Si–O groups) shifted to about 1059 cm^{-1} and was obviously weakened in the spectrum of HEC-*g*-PNaA/MS (Fig. 1c and d). This indicates that MS also participated in the graft copolymerization reaction through its active silanol groups [33,34].

3.2. Thermal behaviours

The TG-DTA curves of HEC, HEC-*g*-PNaA and HEC-*g*-PNaA/MS (10 wt%) were depicted in Fig. 2. It can be noticed that HEC shows one-step thermal decomposition between 277 and 387 °C (weight loss is about 75.9%) after losing its absorbed moisture (about 5.7 wt%). However, the HEC-*g*-PNaA and HEC-*g*-PNaA/MS hydrogels showed three-step continuous thermal decomposition, and the weight-loss rate was obviously slowed. The weight losses of about 14.2 wt% (30–266 °C) for HEC-*g*-PNaA, and about 11.3 wt% (30–270 °C) for HEC-*g*-PNaA/MS correspond to the removal of the absorbed and bonded water. The weight loss of about 20.8 wt% (266–426 °C) for HEC-*g*-PNaA and about 19.1 wt% (270–430 °C) for HEC-*g*-PNaA/MS can be attributed to the dehydration of saccharide rings, the breaking of C–O–C bonds in the chain of HEC and the formation of anhydride with elimination of the water molecule from the two neighboring carboxylic groups of the grafted chains. The weight losses of about 22.9 wt% (426–507 °C) for HEC-*g*-PNaA

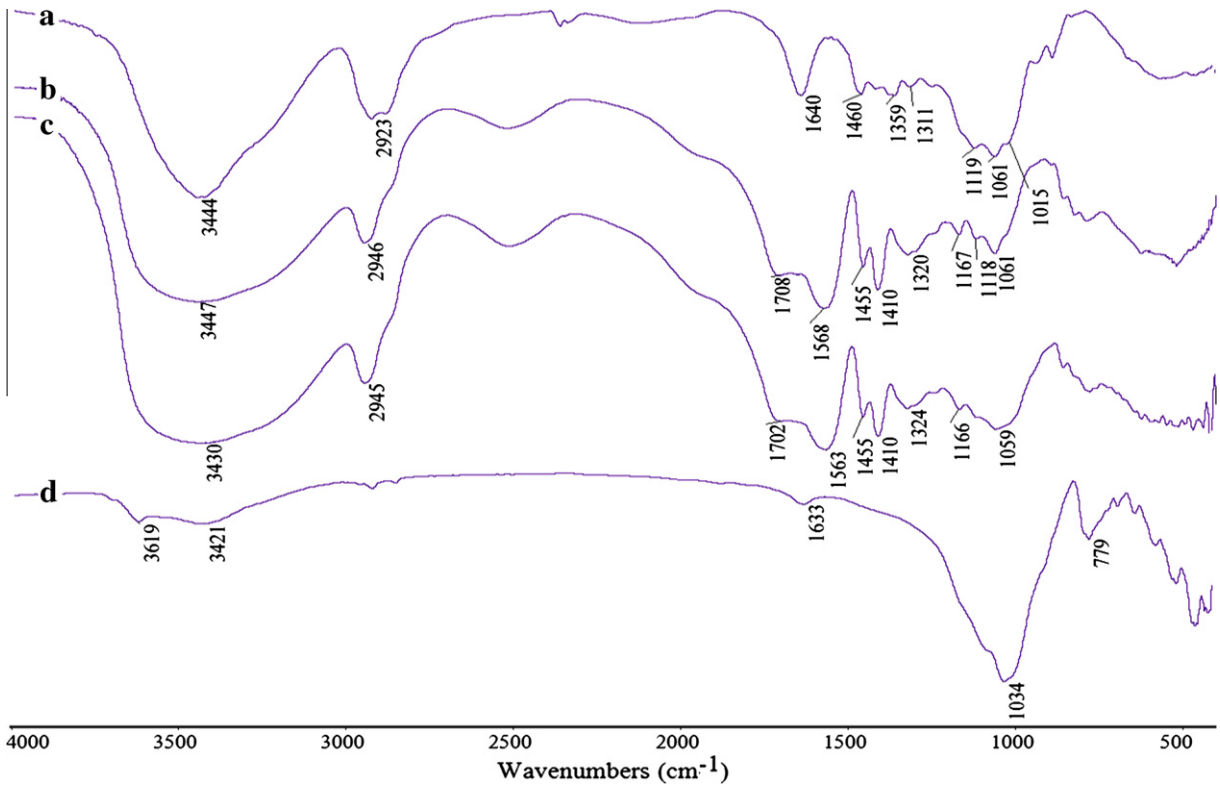

Fig. 1. FTIR spectra of (a) HEC, (b) HEC-*g*-PNaA, (c) HEC-*g*-PNaA/MS and (d) MS.

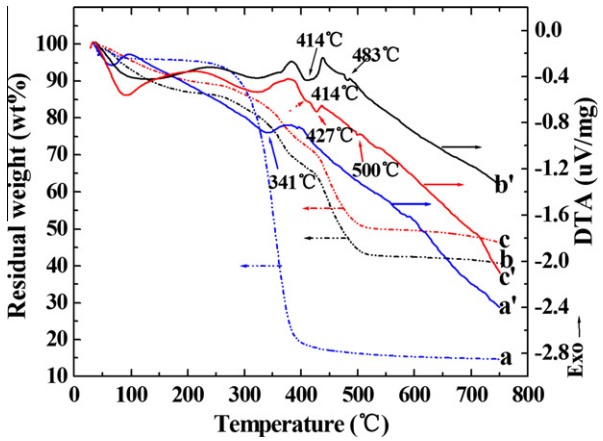

Fig. 2. TG-DTA curves of (a, TG; a′, DTA) HEC-*g*-PNaA, (b, TG; b′, DTA) HEC-*g*-PNaA/MS (10 wt%), and (c, TG; c′, DTA) HEC.

and about 19.8 wt% (430–509 °C) for HEC-*g*-PNaA/MS derive from the breakage of PNaA chains and the destruction of crosslinked network structure. DTA curves confirmed the TG results, and the HEC-*g*-PNaA/MS composite hydrogel is more thermal resistant than HEC and HEC-*g*-PNaA hydrogel. HEC shows an obvious endothermic peak at 342 °C, and HEC-*g*-PNaA hydrogel shows characteristic endothermic peaks at 414 °C and 483 °C, respectively. After introducing MS, these peaks were weakened and shifted to 427 °C and 500 °C, respectively, which indicates that the thermal decomposition process in these regions was relieved. Compared with the HEC-*g*-PNaA hydrogel, the shift of endothermic peaks to high temperature region in the DTA curves reveals that the thermal decomposition of the hydrogel was delayed after incorporating MS. As described above, HEC-*g*-PNaA/MS composite exhibited slower weight-loss and thermal decomposition rate, which indicated the incorporation of MS improved the thermal stability of the hydrogel.

3.3. FESEM, EDS, EM and TEM analyses

The FESEM micrographs of the HEC-*g*-PNaA hydrogel, MS and HEC-*g*-PNaA/MS (10 wt%) composite hydrogel were observed (Fig. 3). It is obvious that the MS-free hydrogel only shows a dense, smooth and non-porous surface. After introducing MS, the surface becomes coarse and loose, and many creases can be observed. The coarse and porous surface contributes the aqueous fluid to diffuse into the polymeric network and affords the final hydrogel with higher swelling capacity [35]. This observation also gives a direct revelation that the MS filler are almost embedded within HEC-*g*-PNaA polymeric matrix and equably dispersed in the matrix without aggregation, which facilitates the resulting superabsorbent to form a homogeneous composition.

Fig. 4 shows the EDS spectrograms of HEC-*g*-PNaA, MS and HEC-*g*-PNaA/MS (10 wt%). It can be seen that only the characteristic peaks of C, O and Na elements appeared in the EDS spectrogram of HEC-*g*-PNaA. After forming HEC-*g*-PNaA/MS composite, the characteristic peaks of Na, Mg, Al, Si, K, Ca and Fe elements (ascribed to MS) can also be observed (Fig. 4b and c). This indicates that MS is existed in the composite hydrogel. For proving the distribution of MS, the elemental maps (EM) for each sample (Fig. 5) were examined and the TEM image (Fig. 6) was observed. It is obvious that the characteristic O, Na, Mg, Al, Si, K, Ca and Fe elements of MS can be clearly observed in the elemental map of the composite hydrogel with an equal distribution. In addition, the TEM image of the HEC-*g*-PNaA/MS composite hydrogel (Fig. 6) shows MS platelets were clearly observed in the polymeric matrix with a better

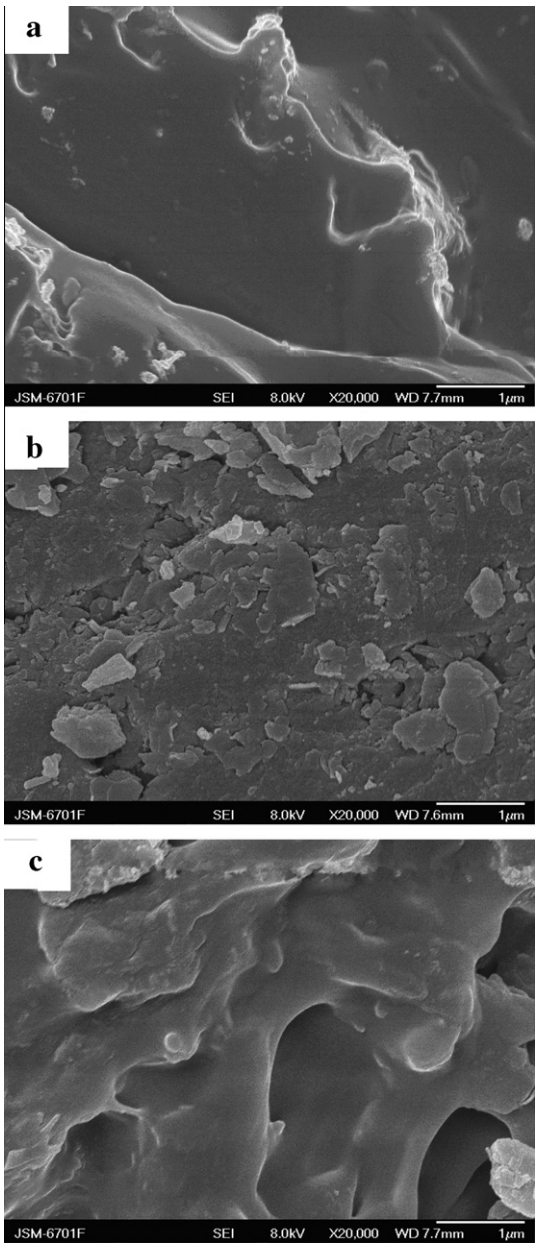

Fig. 3. FESEM micrographs of (a) HEC-*g*-PNaA, (b) MS and (c) HEC-*g*-PNaA/MS (10 wt%).

dispersion, which indicates that MS was existed and distributed in the HEC-*g*-PNaA matrix.

3.4. Effect of MS content on swelling capacity

The structure and composition of the composite hydrogel can be changed by the addition of various amounts of MS, and so its swelling capacity was certainly affected. As shown in Fig. 7, the swelling capacity sharply increased by 400% with the content of MS reaching 10 wt%, and then decreased with the further addition of MS. The encouraging improvement of swelling capacity can be attributed to the following reasons: (1) MS may participate in polymerization reaction through its active silanol groups, which contributes to the formation of regular polymer network, prevents intertwining of grafted polymeric chains and weakens the hydrogen-bonding interaction amongst hydrophilic groups. As a result, the physical crosslinking degree was decreased and the swelling

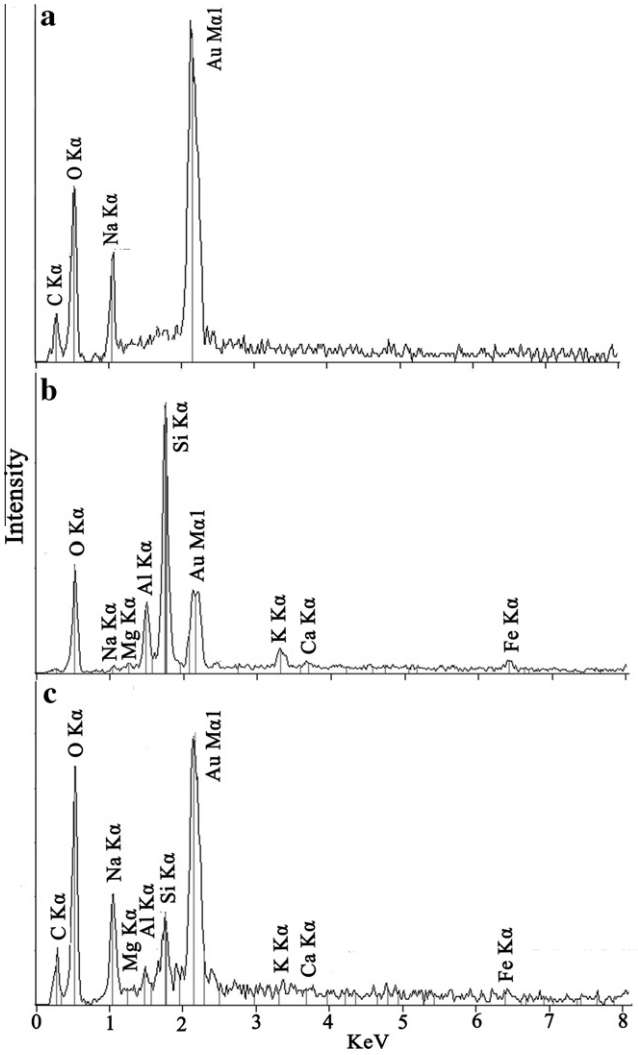

Fig. 4. EDS curves of (a) HEC-*g*-PNaA, (b) MS, (c) HEC-*g*-PNaA/MS (10 wt%).

capacity was notably improved; (2) MS can easily be ionized as contacting with water to release lots of metal cations and generate $[-SiO]^-$ groups [32]. For one thing, the concentration of electrolyte in gel network was increased and the osmotic pressure difference between gel network and swelling media was enhanced; For another, the negatively charged $[-SiO]^-$ can repulse with the negatively charged graft polymer chains, and so the expansion degree of gel network was enhanced. This factor is responsible for the improvement of swelling capacity.

However, the excess MS is physically stacked in the gel network when the addition amount of MS exceeding 10 wt%. The network voids for holding water was obstructed and the hydrophilicity of the hydrogel was decreased, which directly induced the decrease of swelling capacity. In addition, it is worth pointing out that the swelling capacity of the composite hydrogel incorporating with 50 wt% of MS is still higher 117% than the MS-free sample, which is favorable to reduce the production cost.

3.5. Swelling kinetics

Fig. 8a–c depicted the effects of MS content, particle sizes and saline solutions on the swelling kinetics of the hydrogels. It was noticed that the swelling rate is faster at initial 600 s. With prolonging the swelling time, the swelling rate was slowed down until a plateau was reached. In this section, Schott's second-order swelling kinetics model (Eq. (2)) [36] was introduced for evaluating the kinetic swelling behaviours of the hydrogels.

$$t/Q_t = 1/K_{is} + 1/Q_\infty t \quad (2)$$

Here, Q_t (g/g) is the swelling capacity of the hydrogel at time t (s); Q_∞ (g/g) is the theoretical equilibrium swelling capacity, and K_{is} (g/g s) is the initial swelling rate constant. Based on the swelling data in distilled water and saline solutions, the plots of t/Q_t versus t give perfect straight lines with good linear correlation coefficient (>0.99; Fig. 8a'–c'), indicating that the Schott's swelling theoretical model is suitable for evaluating the kinetic swelling behaviours of the composite hydrogels. Also, by the slope and intercept of each straight plot, the swelling kinetic parameters including Q_∞ and K_{is} can be calculated (Table 1). It can be concluded from Table 1 that the initial swelling rate in distilled water for each sample is as following orders: HEC-*g*-PNaA/MS (10 wt%) > HEC-*g*-PNaA/MS (5 wt%) > HEC-*g*-PNaA > HEC-*g*-PNaA/MS (50 wt%), indicating that the introduction of moderate amount of MS is favorable to improve the swelling rate of the hydrogel.

It was also noticed that the initial swelling rate constant (K_{is}) of the HEC-*g*-PNaA/MS (10 wt%) composite hydrogel in distilled water is clearly larger than that in saline solution, and the K_{is} rapidly decreased from 8.1887 to 0.7852 with enhancing the external saline concentration from 0 to 20 mmol/L. This is because the increase of external ionic strength directly decreased the osmotic pressure difference between gel network and external solution. As described previously [37], the net osmotic pressure (π_{ion}) can be determined by Donnan equilibrium theory:

$$\pi_{ion} = RT\sum_i (C_i^g - C_i^s) \quad (3)$$

where C_i is the mobile ion concentration of species i; "g" and "s" denotes the gel and solution phase, respectively. Because the ion concentration in the gel network (C_i^g) is changeless for a hydrogel, the increase of the concentration of saline solution (C_i^s) certainly leads to the decrease of net osmotic pressure (π_{ion}). At the initial stage of swelling, the diffusion of water into polymeric network is the rate-limiting process, and the osmotic pressure difference act as a driving force for this process. So, increasing the external saline concentration certainly induces the decrease of diffusion rate of water molecules.

Apart from saline solution, the particle sizes of the composite hydrogel have greater influence on the swelling rate. As shown in Table 1, the initial swelling rate constant for the HEC-*g*-PNaA/MS (10 wt%) composite hydrogel with different particle sizes follows the orders: 160–200 mesh > 120–160 mesh > 80–120 > 40–80 mesh. This indicates that decreasing the particle size contributes to enhance the swelling rate of the composite hydrogel.

3.6. pH-responsive characteristic

As shown in Fig. 9, the HEC-*g*-PNaA hydrogel and HEC-*g*-PNaA/MS composite hydrogel almost does not swell at pH 2.0, but they rapidly absorb water when it was contacted with pH 7.4 solution. When the swollen gel was immersed in pH 2.0 solution again, the gels were rapidly deswelled and shrinked, and an intriguing pulsatile and on-off switching pH-sensitive behaviours were observed. This is because that the hydrogels contain numerous $-COO^-$ and –COOH groups in its network structure. In pH 2.0 solution, $-COO^-$ groups can convert to –COOH groups, which increased the hydrogen-bonding interaction amongst hydrophilic groups and enhanced the physical crosslinking degree, and so the swelling capacities of the hydrogels are low. When the pH value was changed as 7.4, the opposite process occurred, and the hydrogen-bonding interaction amongst hydrophilic groups was broken, and the

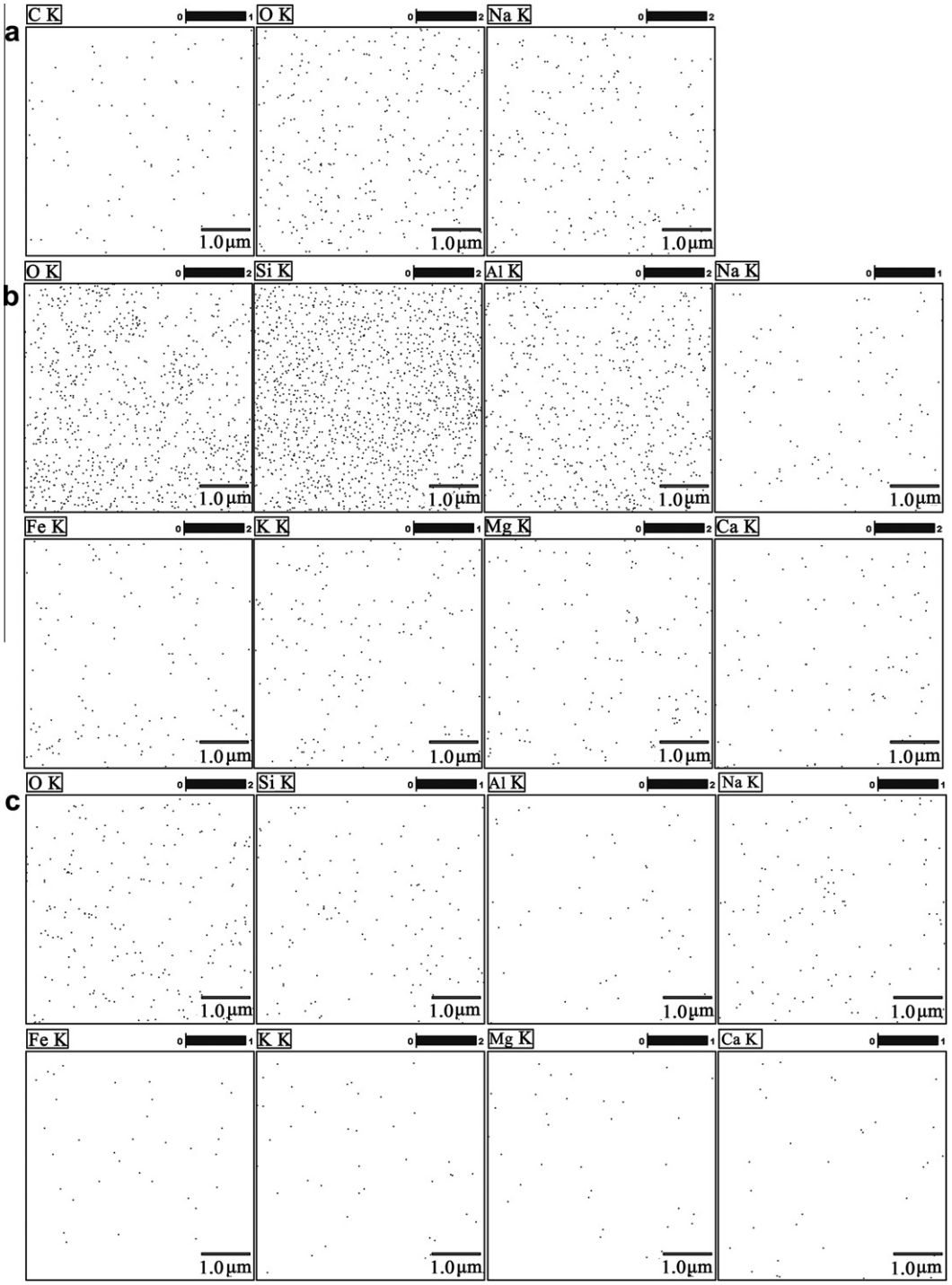

Fig. 5. Element area profiles of (a) HEC-*g*-PNaA, (b) MS, and (c) HEC-*g*-PNaA/MS (10 wt%) at the magnification of 20,000×. The small plots denote the distribution of each element in the polymeric matrix.

electrostatic repulsion amongst polymer chains was increased. As a result, the hydrogels can swell more. It is obvious that the composite hydrogel can recover to relatively higher swelling capacity at pH 7.4 than HEC-*g*-PNaA hydrogel, and more wide responsive region was realized. This indicates that the introduction of MS greatly expanded the responsive region and improved the responsive properties of the hydrogel. After five swelling–deswelling (on–off) cycles between pH 7.4 and 2.0, the composite hydrogel still showed better responsivity, indicating that the pH-sensitivity is highly reversible.

3.7. Saline-responsive characteristic

The swelling–deswelling switching cycle of the optimized composite hydrogel was examined by alternately contacting it with 0.9 wt% NaCl solution and distilled water for a set interval (Fig. 10). In 0.9 wt% NaCl solution, the composite hydrogel shows low swelling capacity (about 80 g/g), and the composite gel keeps smaller volume. However, when the above gel was immersed in distilled water, the gel rapidly expands and absorbs large amounts of water with prolonging time. After the swollen composite was

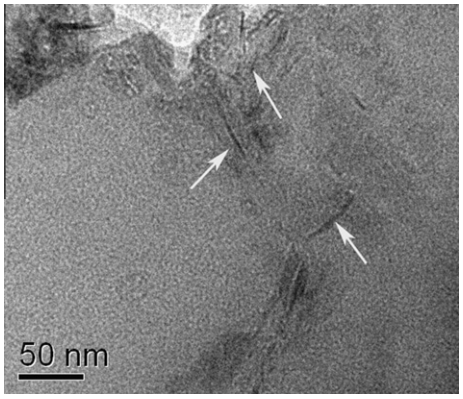

Fig. 6. TEM image of the HEC-g-PNaA/MS (10 wt%) composite hydrogel.

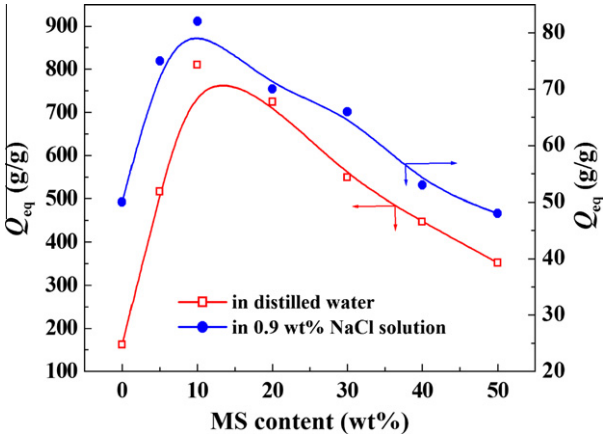

Fig. 7. Effects of MS content on the swelling capacity in distilled water and 0.9 wt% NaCl solution.

Table 1
Swelling kinetic parameters for the hydrogels in distilled water and saline solutions with various concentrations.

Samples	Particle sizes (mesh)	Swelling media	Q_∞ (g/g)	K_{is} (g/g s)	R^a
HEC-g-PNaA	40–80	Distilled water	158	1.5261	0.9998
HEC-g-PNaA/MS (5 wt%)	40–80	Distilled water	568	3.1989	0.9993
HEC-g-PNaA/MS (10 wt%)	40–80	Distilled water	830	8.1887	0.9998
HEC-g-PNaA/MS (50 wt%)	40–80	Distilled water	345	1.5234	0.9999
HEC-g-PNaA/MS (10 wt%)	40–80	2 mmol/L NaCl	474	3.1411	0.9999
HEC-g-PNaA/MS (10 wt%)	40–80	5 mmol/L NaCl	308	2.2773	0.9999
HEC-g-PNaA/MS (10 wt%)	40–80	10 mmol/L NaCl	258	1.4717	0.9998
HEC-g-PNaA/MS (10 wt%)	40–80	20 mmol/L NaCl	201	0.7852	0.9993
HEC-g-PNaA/MS (10 wt%)	80–120	Distilled water	788	8.6244	0.9998
HEC-g-PNaA/MS (10 wt%)	120–160	Distilled water	746	9.7809	0.9999
HEC-g-PNaA/MS (10 wt%)	160–200	Distilled water	730	11.0266	0.9999

[a] The regression equation for each sample is $Y = A + Bx$ ($Y = t/Q_t$, $A = 1/K_{is}$, $B = 1/Q_\infty$, $x = t$).

transferred into 0.9 wt% NaCl solution again, it rapidly de-swells and shrinks to a smaller volume. This is because the addition of Na^+ cations decreased the osmotic pressure difference between gel network and external solution, which decreased the driving force for the penetration of water molecules, and so the composite show low swelling capacity in 0.9 wt% NaCl solution. As the shrunken composite was immersed in fresh distilled water again, some of Na^+ cations was washed out and the osmotic pressure was recovered, and so the swelling capacity reached relatively higher value. It can also be observed that the swelling capacity only lost

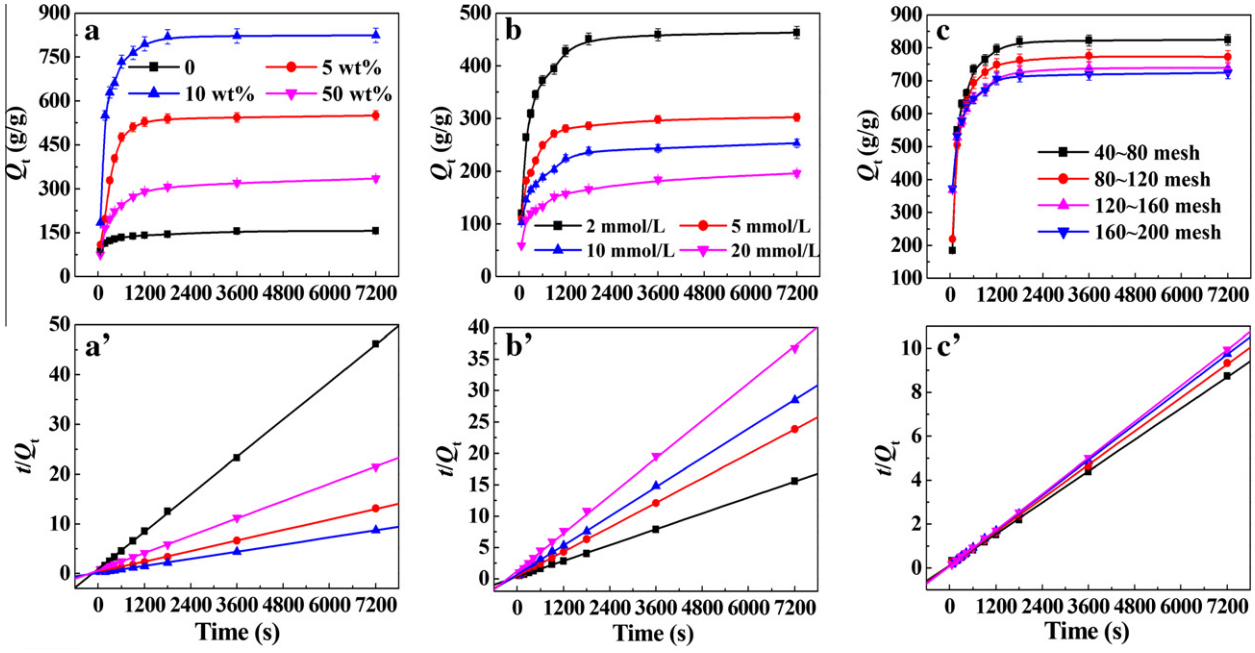

Fig. 8. (a) swelling kinetic curves of the hydrogels (MS dosage, 0, 5, 10 and 50 wt%) in distilled water, (b) effect of the saline solution with various concentration on the kinetic swelling behaviours of the composite hydrogel (MS dosage, 10 wt%), and (c) effect of particle size on the kinetic swelling behaviours of the composite hydrogel (MS dosage, 10 wt%); a′–c' are the corresponding plots of t/Q_t against t for a–c.

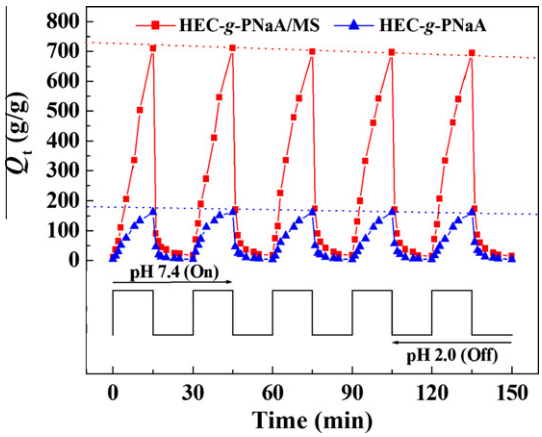

Fig. 9. The On–Off switching swelling behaviour as reversible pulsatile swelling (pH 7.4) and deswelling (pH 2.0) of the HEC-*g*-PNaA hydrogel and the HEC-*g*-PNaA/MS (10 wt%) composite hydrogel. The area between two dashed lines denotes the extended responsive region.

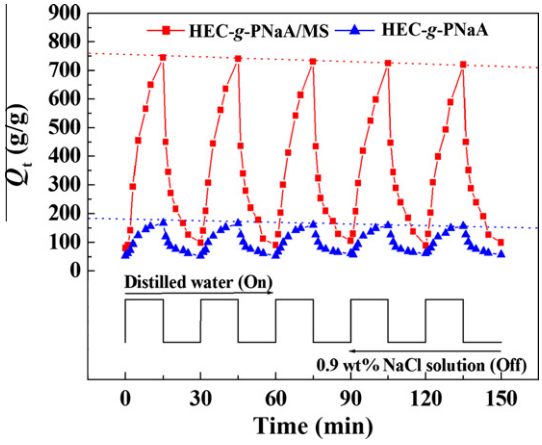

Fig. 10. The On–Off switching swelling behaviour as reversible swelling (in distilled water) and deswelling (in 0.9 wt% NaCl solution) of the HEC-*g*-PNaA hydrogel and the HEC-*g*-PNaA/MS (10 wt%) composite hydrogel. The area between two dashed lines denotes the extended responsive region.

little even after five cycles, and the reversible swelling–deswelling (On–Off) behaviours were realized. The evident On–Off switchable swelling behaviour with altering the external saline media presented the excellent saline-responsive characteristic of the composite hydrogel. It can especially be noticed that the composite hydrogel can recover to relatively higher swelling capacity in distilled water than HEC-*g*-PNaA hydrogel, and the On–Off switching effect is more obvious and the responsive behaviours is more strong. This indicates that the introduction of MS greatly expanded the saline-responsive region of the hydrogel, and which is favorable to its application as a stimuli-sensitive material.

3.8. Effects of surfactants on the swelling behaviour

Apart from the saline solution, ionic surfactants have a considerable effect on the swelling properties of the hydrogels. As shown in Fig. 11, the swelling capacity of the composite hydrogel decreased with increasing the concentration of surfactant NaOL and DTAB, but the decreasing trend in the DTAB solution is more obvious than in the NaOL solution. At the concentration of 20 mmol/L, the swelling capacity of the composite in NaOL solution reaches 247 g/g, but it is only 33 g/g in DTAB solution. This indicates that the swelling capacity is highly dependent on the concentration and charge of the solution of surfactants. In DTAB solution, the –COOH groups of the composite hydrogel may form a strong hydrogen bond with the quaternary ammonium cations of DTAB, and the negatively charged $–COO^-$ groups may generate electrostatic interaction with positively charged DTA^+ moieties. In addition, the DTAB molecules may aggregate within or over the networks of composites, which can markedly decrease the hydrophilicity of the polymer network and reduce the swelling capacity [38]. However, no similar action occurred when the composite was immersed in the solution of anionic surfactant NaOL. As a result, the composite showed a comparatively faster deswelling rate in the cationic surfactant solution than in the anionic surfactant solution.

3.9. Effects of hydrophilic organic solvents on swelling behaviour

Effects of hydrophilic organic solvents on the swelling behaviours of the hydrogel have attracted great interests because of the intriguing gel phase transition. Fig. 12 shows the swelling curves of the hydrogel in the aqueous solution of methanol, acetone and dimethyl sulfoxide (DMSO) at various concentrations. It can be seen that the swelling capacity slowly decreased with increasing the concentration of methanol or acetone at the low concentration range (<50 vol% for methanol; <40 vol% for acetone), but the gel rapidly de-swells with increasing the concentration of methanol (>50 vol%) and acetone (>40 vol%) solution, until the gel completely collapsed at the concentration of 70 vol% for methanol and 60 vol% for acetone. However, a distinct trend was observed in the aqueous solution of DMSO. The swelling capacity initially increased with increasing the concentration of DMSO, and a maximum absorption was achieved at 20 vol%, and a similar trend was also observed in previous work [39]. The experiments were repeated for several times, and the "overflowing" behaviour is reproducible. The solvent-induced swelling-loss of the hydrogels can be explained by the Hildebrand equation (Eq. (4)) [40].

$$\Delta H_m/(V_m\Phi_1\Phi_2) = (\delta_1 - \delta_2)^2 \quad (4)$$

where ΔH_m is the enthalpy change upon mixing of a polymer and a solvent, V_m is the whole volume of the solution, Φ_1 and Φ_2 are the volume fractions for the solvent and the polymer, δ_1 and δ_2 are the solubility parameters for the solvent and the polymer, respectively. It can be noticed from Eq. (4) that the swelling degree of hydrogel depends on its solubility in swelling media. Because the

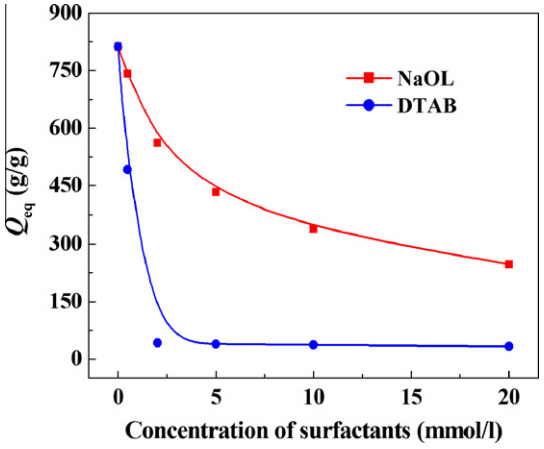

Fig. 11. Effects of surfactant solutions on the swelling behaviour of the HEC-*g*-PNaA/MS (10 wt%) composite hydrogel.

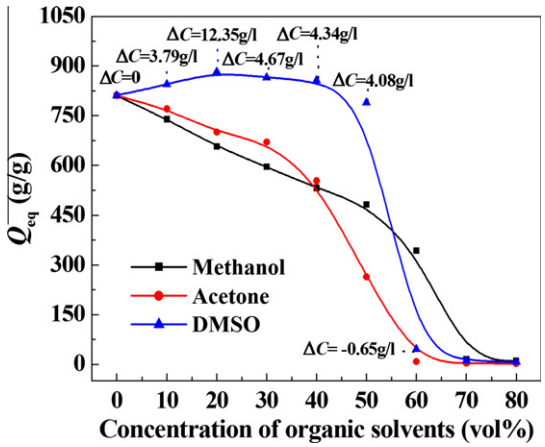

Fig. 12. Effects of hydrophilic organic solvents on the swelling behaviour of the HEC-g-PNaA/MS (10 wt%) composite hydrogel.

maximum swelling capacity of the hydrogel is often obtained in pure water, the δ value of water $(23.4\,(cal/cm^3)^{1/2})$ can be regarded as the solubility parameter of the hydrogel. The solubility parameter for a mixing solution (δ_{mix}) can be calculated using Eq. (5) [40]:

$$\delta_{mix} = \delta_1 \Phi_1 + \delta_2 \Phi_2 \tag{5}$$

where Φ_1 and Φ_2 are the volume fraction for the two components, and δ_1 and δ_2 are the solubility parameters of each component. The δ values of methanol, acetone and DMSO are 14.5, 9.9 and $14.5\,(cal/cm^3)^{1/2}$, respectively, which is clearly smaller than 23.4 of water. Thus, the addition of methanol and acetone (poor solvent for the hydrogel) may induce the decrease of swelling capacity. It can also be calculated that the δ value for the hydrogel beginning to collapse is $18.95\,(cal/cm^3)^{1/2}$ for methanol, $18\,(cal/cm^3)^{1/2}$ for acetone and $18.95\,(cal/cm^3)^{1/2}$ for DMSO. Apart from solubility parameters, the dielectric constant of the solution directly affects the ionization degree of ionic groups, and then changes the difference of ion concentrations between gel network and external solution [41]. As a result, the swelling capacity can be affected. The dielectric constant of binary mixture solution can be calculated by Eq. (6).

$$\varepsilon_{mix} = 78.54\psi_1 + \varepsilon_2\psi_2 \tag{6}$$

where ψ_1 and ψ_2 denote the volume fractions of water and organic solvents, respectively, and ε_2 represent the dielectric constants of organic solvents. The dielectric constants of water, methanol, acetone and DMSO are 78.54, 32.63, 20.7 and 47, respectively [39,41]. The addition of methanol or acetone certainly decreases the dielectric constants of the mixture solutions, and the dissociation of –COOH and $–COO^-$ groups was restrained, and so the swelling capacity also exhibits a similar decreasing tendency with increasing the concentration of methanol or acetone.

However, in the aqueous solution of DMSO, the additional hydrogen-bonding interaction between the gel network and DMSO molecules makes the swelling "overflowing". In aqueous solution of DMSO, the DMSO molecules may enter the gel network and form hydrogen bonding with the hydrophilic groups [39]. Thus, numerous DMSO molecules may reside in the interior of gel network. For proving this, the concentration of DMSO in the internal gel network and external solution was determined by X-ray fluorescence (XRF) technique. The concentration differences (ΔC) between swollen gel network and external solution are 3.79 (10 vol%), 12.35 (20 vol%), 4.67 (30 vol%), 4.34 (40 vol%), 4.08 (50 vol%) and −0.65 (60 vol%) g/l. When the initial concentration of DMSO solution is lower than 50 vol%, the DMSO concentration in internal gel network is higher than that in external solution (the DMSO was denoted as a solute), and an additional osmotic pressure $\Delta\Pi_{org}$ generated (Scheme 1) [41]. Under this condition, the comprehensive contribution of additional osmotic pressure $\Delta\Pi_{org}$ to enhancing the swelling capacity is larger than the decreasing effect of the solubility parameter and dielectric constant on swelling capacity. As a result, the swelling capacity was enhanced after adding moderate amount of DMSO in aqueous solution. But the further increase of the external concentration of DMSO leads to the disappearance of concentration difference of DMSO, and the effect of the solubility parameter and dielectric constant is dominant, and so the swelling gel rapidly collapsed when DMSO concentration is higher than 50 vol%.

4. Conclusions

In efforts to reduce the consumption of petroleum products and the environmental impact resulting from industrial polymers and to expand the application domain of hydrogels, new types of biopolymer-based composite hydrogels with pH- and saline-responsive characteristics, improved swelling capacity and rate were prepared by free-radical solution polymerization amongst HEC, NaA, MS and MBA. FTIR, TG-DTA, FESEM, EDS, EM and TEM analyses revealed that the NaA monomers have been grafted onto the HEC backbone, and the surface porosity, roughness and

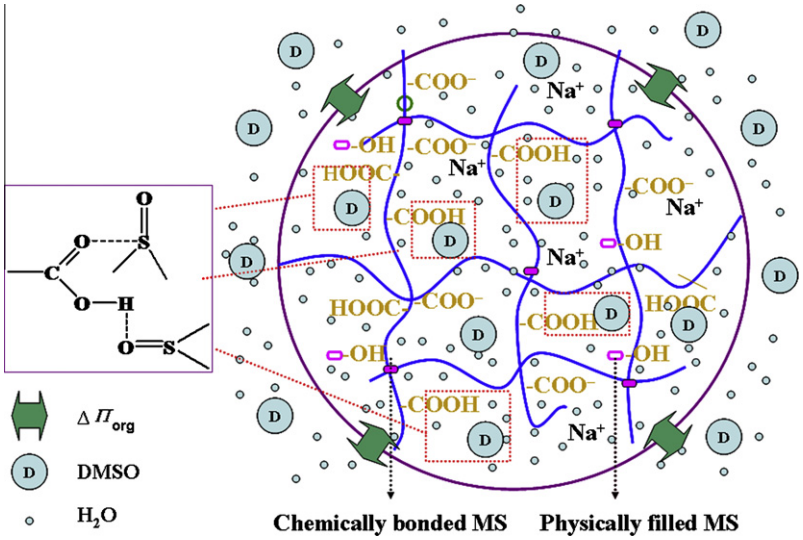

Scheme 1. Schematic illustration of the interaction of DMSO with the gel network.

thermal stability of the hydrogel were improved after incorporating MS. MS existed in the composite hydrogel and led to a better dispersion in the polymer matrix. The incorporation of 10 wt% MS greatly enhanced the swelling capacity by 400% and the initial swelling rate constant also enhanced 7.48 fold in contrast to the MS-free sample. Even when the content of MS reached 50 wt%, the swelling capacity also enhanced almost by 117%. This is favorable to reduce the production cost because the mass ratio of cheap inorganic MS to other organic components in the composite reached 1:1. The swelling kinetic results showed that the swelling rate of the composite decreased with increasing the external saline concentration and the particle size. The composite hydrogel exhibited highly reversible On–Off switchable stimuli-responsive behaviours between pH 7.4 and 2.0 solutions, and between distilled water and 0.9 wt% NaCl solutions, and the responsive region of the hydrogel was drastically expanded after introducing 10 wt% MS. In addition, the composite showed anticipated deswelling behaviours in various surfactant solutions, and the deswelling trend is more clearly in the solutions of cationic surfactant DTAB than that in the solution of anionic surfactant NaOL. In DMSO solution, the hydrogel shows intriguing "overflowing" swelling behaviour in contrast to that in methanol and acetone solution, which may be ascribed to the generation of additional osmotic pressure. In short, the composite hydrogels based on renewable, non-toxic and biodegradable HEC and abundant MS showed enhanced swelling capability and rate, excellent pH- and saline-responsive properties and better deswelling capability in aqueous solutions of various surfactants, which can be used as potential water-manageable materials and as a candidate for petroleum-based synthetic absorbents.

Acknowledgments

The authors thank for jointly supporting by the National Natural Science Foundation of China (No. 20877077) and "863" Project of the Ministry of Science and Technology, PR China (No. 2006AA100215).

References

[1] Ray SS, Bousmina M. Biodegradable polymers and their layered silicate nanocomposites: in greening the 21st century materials world. Prog Mater Sci 2005;50:962–1079.
[2] Darder M, Colilla M, Ruiz-Hitzky E. Biopolymer-clay nanocomposites based on chitosan intercalated in montmorillonite. Chem Mater 2003;15:3774–80.
[3] Delhom CD, White-Ghoorahoo LA, Pang SS. Development and characterization of cellulose/clay nanocomposites. Compos B: Eng 2010;41:475–81.
[4] Das A, Kothari VK, Makhija S, Avyaya K. Development of high-absorbent lightweight sanitary napkin. J Appl Polym Sci 2007;107:1466–70.
[5] Teodorescu M, Lungu A, Stanescu PO, Neamtu C. Preparation and properties of novel slow-release NPK agrochemical formulations based on poly(acrylic acid) hydrogels and liquid fertilizers. Ind Eng Chem Res 2009;48:6527–34.
[6] Guilherme MR, Reis AV, Paulino AT, Moia TA, Mattoso LHC, Tambourgi EB. Pectin-based polymer hydrogel as a carrier for release of agricultural nutrients and removal of heavy metals from wastewater. J Appl Polym Sci 2010;117:3146–54.
[7] Kaşgöz H, Durmus A, Kaşgöz A. Enhanced swelling and adsorption properties of AAm-AMPSNa/clay hydrogel nanocomposites for heavy metal ion removal. Polym Adv Technol 2008;19:213–20.
[8] Tang QW, Sun XM, Li QH, Wu JH, Lin JM. Synthesis of polyacrylate/polyethylene glycol interpenetrating network hydrogel and its sorption of heavy-metal ions. Sci Technol Adv Mater 2009;10:015002. 7pp.
[9] Kandile NG, Nasr AS. Environment friendly modified chitosan hydrogels as a matrix for adsorption of metal ions, synthesis and characterization. Carbohyd Polym 2009;78:753–9.
[10] Li P, Siddaramaiah, Kim NH, Heo SB, Lee JH. Novel PAAm/Laponite clay nanocomposite hydrogels with improved cationic dye adsorption behavior. Compos B: Eng 2008;39:756–63.
[11] Tang QW, Lin JM, Wu ZB, Wu JH, Huang ML, Yang YY. Preparation and photocatalytic degradability of TiO_2/polyacrylamide composite. Eur Polym J 2007;43:2214–20.
[12] Kangwansupamonkon W, Jitbunpot W, Kiatkamjornwong S. Photocatalytic efficiency of TiO_2/poly[acrylamide-*co*-(acrylic acid)] composite for textile dye degradation. Polym Degrad Stabil 2010;9:1894–902.
[13] Sadeghi M, Hosseinzadeh H. Synthesis of starch-poly(sodium acrylate-*co*-acrylamide) superabsorbent hydrogel with salt and pH-responsiveness properties as a drug delivery system. J Bioact Compat Polym 2008;23:381–404.
[14] Pourjavadi A, Barzegar S. Synthesis and evaluation of pH and thermosensitive pectin-based superabsorbent hydrogel for oral drug delivery systems. Starch-Stärke 2009;61:161–72.
[15] Cheung HY, Lau KT, Lu TP, Hui D. A critical review on polymer-based bio-engineered materials for scaffold development. Compos B: Eng 2007;38:291–300.
[16] Mahdavinia GR, Pourjavadi A, Hosseinzadeh H, Zohuriaan MJ. Modified chitosan 4. Superabsorbent hydrogels from poly(acrylic acid-*co*-acrylamide) grafted chitosan with salt- and pH-responsiveness properties. Eur Polym J 2004;40:1399–407.
[17] Tang QW, Lin JM, Wu JH, Xu YW, Zhang CJ. Preparation and water absorbency of a novel poly(acrylate-*co*-acrylamide)/vermiculite superabsorbent composite. J Appl Polym Sci 2007;104(2):735–9.
[18] Li P, Kim NH, Siddaramaiah, Lee JH. Swelling behavior of polyacrylamide/laponite clay nanocomposite hydrogels: pH-sensitive property. Compos B: Eng 2009;40:275–83.
[19] Al E, Güçlü G, yim TB, Emik S, Özgümüş S. Synthesis and properties of starch-*graft*-acrylic acid/Na-montmorillonite superabsorbent nanocomposite hydrogels. J Appl Polym Sci 2008;109:16–22.
[20] Demitri C, Sole RD, Scalera F, Sannino A, Vasapollo G, Maffezzoli A, et al. Novel superabsorbent cellulose-based hydrogels crosslinked with citric acid. J Appl Polym Sci 2008;110:2453–60.
[21] Šimkovic I. What could be greener than composites made from polysaccharides? Carbohyd Polym 2008;74:759–62.
[22] Kiatkamjornwong S, Chomsaksakul W, Sonsuk M. Radiation modification of swelling capacity of cassava starch by acrylic acid/acrylamide. Radiat Phys Chem 2000;59:413–27.
[23] Pourjavadi A, Ghasemzadeh H, Mojahedi F. Swelling properties of CMC-*g*-poly(AAm-*co*-AMPS) superabsorbent hydrogel. J Appl Polym Sci 2009;113:3442–9.
[24] Pourjavadi A, Ghasemzadeh H, Soleyman R. Synthesis, characterization, and swelling behavior of alginate-g-poly(sodium acrylate)/kaolin superabsorbent hydrogel composites. J Appl Polym Sci 2007;105:2631–9.
[25] Wang WB, Wang AQ. Synthesis and swelling properties of pH-sensitive semi-IPN superabsorbent hydrogels based on sodium alginate-*g*-poly(sodium acrylate) and polyvinylpyrrolidone. Carbohyd Polym 2010;80(4):1028–36.
[26] Chen Y, Liu YF, Tan HM, Jiang JX. Synthesis and characterization of a novel superabsorbent polymer of N,O-carboxymethyl chitosan graft copolymerized with vinyl monomers. Carbohyd Polym 2009;75:287–92.
[27] Wang WB, Wang AQ. Preparation, characterization and properties of superabsorbent nanocomposites based on natural guar gum and modified rectorite. Carbohyd Polym 2009;77:891–7.
[28] Fujioka R, Tanaka Y, Yoshimura T. Synthesis and properties of superabsorbent hydrogels based on guar gum and succinic anhydride. J Appl Polym Sci 2009;114:612–6.
[29] Abd El-Mohdy HL, Abd El-Rehim HA. Radiation synthesis of kappa-carrageenan/acrylamide graft copolymers as superabsorbents and their possible applications. J Polym Res 2009;16:63–72.
[30] Pourjavadi A, Hosseinzadeh H, Sadeghi M. Synthesis, characterization and swelling behavior of gelatin-g-poly(sodium acrylate)/kaolin superabsorbent hydrogel composites. J Compos Mater 2007;41:2057–69.
[31] Lin SB, Wu JH, Yao KD, Cai KY, Xiao CM, Jiang CJ. Study of microstructure and properties of HEC-*g*-AA/SiO_2 organic–inorganic hybrid materials. Compos Interface 2004;11:271–6.
[32] Li J, Zhang PY, Gao Y, Song XG, Dong JH. Overview of Maifanshi: its physi-chemical properties and nutritious function in drinking water. Environ Sci Technol (China) 2008;31(10):63–6. 75.
[33] Li A, Wang AQ, Chen JM. Studies on poly(acrylic acid)/attapulgite superabsorbent composite. I. Synthesis and characterization. J Appl Polym Sci 2004;92:1596–603.
[34] Wu JH, Lin JM, Li GQ, Wei CR. Influence of the COOH and COONa groups and crosslink density of poly(acrylic acid)/montmorillonite superabsorbent composite on water absorbency. Polym Int 2001;50:1050–3.
[35] Santiago F, Mucientes AE, Osorio M, Rivera C. Preparation of composites and nanocomposites based on bentonite and poly(sodium acrylate). Effect of amount of bentonite on the swelling behaviour. Eur Polym J 2007;43:1–9.
[36] Schott H. Swelling kinetics of polymers. J Macromol Sci B: Phys 1992;31:1–9.
[37] Dogu S, Kilic M, Okay O. Collapse of acrylamide-based polyampholyte hydrogels in water. J Appl Polym Sci 2009;113:1375–82.
[38] Mohan YM, Premkumar T, Joseph DK, Geckeler KE. Stimuli-responsive poly(N-isopropylacrylamide-co-sodium acrylate) hydrogels: A swelling study in surfactant and polymer solutions. React Funct Polym 2007;67:844–58.
[39] Kabiri K, Zohuriaan-Mehr MJ, Mirzadeh H, Kheirabadi M. Solvent-, ion- and pH-specific swelling of poly(2-acrylamido-2-methylpropane sulfonic acid) superabsorbing gels. J Polym Res 2010;17:203–12.
[40] Chen JW, Shen JR. Swelling behaviors of polyacrylate superabsorbent in the mixtures of water and hydrophilic solvents. J Appl Polym Sci 2000;75:1331–8.
[41] Liu Y, Xie JJ, Zhu MF, Zhang XY. A study of the synthesis and properties of AM/AMPS copolymer as superabsorbent. Macromol Mater Eng 2004;289:1074–8.